DEVELOPMENT OF BULK GaAs ROOM TEMPERATURE RADIATION DETECTORS

D.S. McGregor*, G.F. Knoll*, Y. Eisen**, and R. Brake†,
*Department of Nuclear Engineering, The University of Michigan, Ann Arbor, MI 48109-2100
**Soreq Nuclear Research Center, Israel Atomic Energy Commission, Yavne 70600, Israel
†Radiation Protection Group, Los Alamos National Laboratory, Los Alamos, NM 87545

Abstract

GaAs is a wide band gap semiconductor with potential use as a room temperature radiation detector. Various configurations of Schottky diode detectors were fabricated with bulk crystals of liquid encapsulated Czochralski (LEC) semi-insulating undoped GaAs material. Basic detector construction utilized one Ti/Au Schottky contact and one Au/Ge/Ni alloyed ohmic contact. Pulsed X-ray analysis indicated pulse decay times dependent on bias voltage. Pulse height analysis disclosed non-uniform electric field distributions across the detectors tentatively explained as a consequence of native deep level donors (EL2) in the crystal. Pulse height spectra measured from an ^{241}Am alpha particle source at room temperature resulted in resolution ranging from 2.2% to 3.1% at FWHM for several detectors with a typical resolution of 2.5%. Low energy gamma rays measured under room temperature operating conditions resulted in observed full energy peaks of 60 keV and 122 keV photons with measured FWHM's of 22 keV and 40 keV, respectively.

I. INTRODUCTION

The band gap of GaAs is 1.42 eV at room temperature and is sufficiently wide to allow for its use as a radiation detector at room temperature [1, 2]. The investigation of GaAs as a detector material dates back to the late 1960s and early 1970s [3, 4, 5]. At that time, bulk GaAs material was of inferior quality by todays standards and the most successful of these early detectors were fabricated from liquid phase epitaxially (LPE) grown GaAs crystals. Unfortunately, LPE grown material was limited to thicknesses of 100 microns or less, thus limiting detector utilization to charged particle or low energy X-ray and gamma-ray spectroscopy. Since that time, high quality semi-insulating liquid encapsulated Czochralski (LEC) GaAs material has become available from a number of commercial suppliers. LEC bulk material provides a potential medium for fabricating thick GaAs detectors at relatively low cost. Compensation of impurities has improved in LEC GaAs such that quoted resistivities and carrier concentrations approach theoretical intrinsic values. The use of bulk GaAs material for detection of radiation has recently undergone renewed interest [6, 7]. Presented in this work are the results from Schottky contact based diode detectors fabricated from commercially available LEC bulk GaAs material.

A. *Material Considerations*

Unlike Si or Ge, GaAs has a direct band gap allowing for direct transitions of electrons from the valence band to the conduction band without a change in momentum. Electrons located in the direct conduction band valley (Γ valley) experience high mobility (above 7000 cm^2/V-s) resulting in high electron velocities at low electric fields. Higher electric fields result in scattering of electrons into a lower mobility valley (L valley) leading to decreased velocity. Thus, electrons obtain a maximum velocity of 2×10^7 cm/s at electric field strengths near 3×10^3 V/cm and reduce to saturated velocities below 1×10^7 cm/s above field strengths of 3×10^4 V/cm. Holes have much lower mobility in GaAs (400 cm^2/V-s) and reach saturated velocities similar to electrons at electric field strengths above 3×10^4 V/cm. Unfortunately, the high electron velocity characteristic of GaAs is not utilized if comparable electron and hole velocities are to be obtained.

Direct band gap transitions of electrons from the conduction band to the valence band cause reduction in carrier lifetimes as compared to Si or Ge. However, theoretical models of the material in which recombination occurs from direct radiative transitions indicate that a very pure crystal should have lifetimes approaching 0.1 ms [8]. To the knowledge of the authors, such long lifetimes have not been demonstrated in GaAs material to date. High densities of trapping centers in GaAs are believed to be the major cause of short carrier lifetimes commonly observed.

GaAs characteristically has a high density of surface states[1] which tend to predetermine (or pin) the Fermi level at the metal-semiconductor interface [9, 10]. The pinning of the Fermi level forces the barrier height to form as

[1] An exception is a clean and well cleaved (110) surface in which surface states do not form in the bulk band gap.

a function of the filled surface state density rather than the metal work function. The fact that the barrier height formed is independent of the metal work function makes altering the barrier height difficult; however, fabrication repeatability of contacts is easily realized. The barrier height has been reported to pin at approximately 2/3 of the band gap energy for n-type material and 1/3 of the band gap energy for p-type material.

Bulk LEC GaAs is semi-insulating due to compensation of carbon impurities in the material by the native arsenic antisite defect EL2 [11, 12]. The native defect EL2 acts as a deep donor level and is not fully ionized at room temperature. Residual carbon acceptor impurities are almost completely ionized at room temperature and generally render LEC GaAs material p-type. It is necessary that the concentration of compensating deep levels be greater than the net concentration of compensated shallow impurities if semi-insulating material is to be realized [13]. In the case of EL2 deep donor compensation of carbon acceptor impurities, the conditions for semi-insulating behavior in undoped LEC GaAs are

$$N_a > N_d \tag{1}$$

and

$$N_{DD} > N_a - N_d \tag{2}$$

where N_{DD} is the deep donor concentration, N_a is the shallow acceptor concentration, and N_d is the shallow donor concentration. Although carbon impurities are significantly reduced, a low concentration of carbon is allowed to remain in the GaAs melt in order to meet the criteria in equations 1 and 2. Additionally, semi-insulating GaAs is grown slightly arsenic rich in order to produce the proper concentration of deep donor EL2 sites throughout the crystal. GaAs ingots are commonly annealed after growth in order to improve the uniformity of the resistivity throughout the material. The resulting GaAs has typical free carrier concentrations of $10^7/\text{cm}^3$ and resistivities greater than 10^7 Ω-cm. The density of EL2 sites are typically quoted near $10^{16}/\text{cm}^3$ and the density of carbon acceptors are typically quoted near $5 \times 10^{14}/\text{cm}^3$. Discussion of problems arising from the presence of the EL2 donors and carbon impurities is provided later in the text (section IV.).

The average density (5.32 g/cm^3) and atomic number (31/33) of GaAs are approximately the same as Ge, the most commonly used semiconductor for high resolution gamma ray spectroscopy. Therefore the gamma ray interaction probabilities per unit path length are approximately the same. The energy required to create an electron-hole pair (ϵ) is 4.2 eV and the Fano factor (F) has been reported to be 0.18 [14]. The theoretical energy resolution obtainable for GaAs at full width at half maximum (FWHM) calculated from

$$R_E = 2.35\sqrt{EF\epsilon} \tag{3}$$

where E is the gamma ray energy indicates that acceptably high resolution for gamma ray spectroscopy can be obtained. However, problems with statistical fluctuations in carrier extraction from varying mechanisms have prevented the realization of high resolution gamma ray spectroscopy in bulk GaAs material to date.

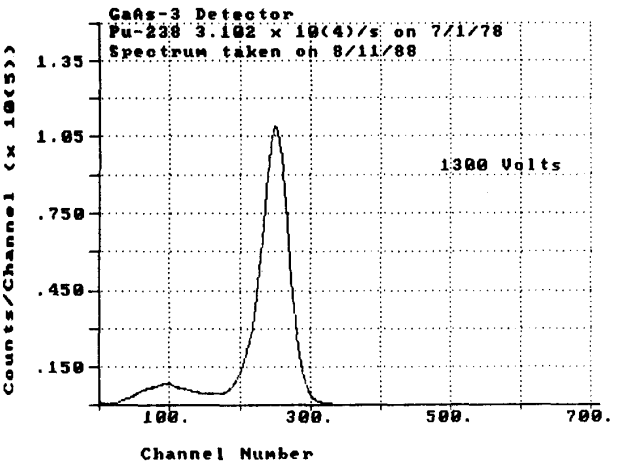

Figure 1: Spectrum of ^{238}Pu 5.5 MeV Alpha Particles Measured with an Early Generation Schottky-Schottky Bulk GaAs Detector.

B. *Previous LEC GaAs Detectors*

Early detectors fabricated from LEC bulk material suffered severe surface leakage currents and full energy peaks were not observed [15]. However, the leakage current could be greatly decreased by introducing traps through surface damage. Later generation back to back Schottky diodes fabricated from 500 micron thick bulk GaAs material showed full energy peaks from alpha particles with FWHM's of 15% (Figure 1). The noise level from the Schottky-Schottky devices was observed to be 300 keV. Charge collection efficiency ranged from 30% to 35% as compared to a silicon surface barrier detector, thus indicating severe trapping of charge carriers. Statistical fluctuations in carrier extraction due to the forward biased Schottky contact and carrier trapping are believed to have contributed to the poor resolution observed.

Reduction of noise to 50 keV was accomplished by substituting one alloyed ohmic contact for the forward biased Schottky contact. Low energy gamma rays were observed only as a plateau continuum (as shown in Figure 2), and the devices performed as photon counters rather than spectrometers. The continuum end point energy was observed to increase linearly with gamma ray energy, indicating a linear production of electron-hole pairs with energy. The absence of gamma ray full energy peaks in these early devices is believed to be resultant from severe carrier trapping in inferior bulk material. Conversion electrons and beta particles were observed from a ^{137}Cs beta particle source with the same GaAs devices (Figure 3). Resolution of alpha particle irradiation ranged from 5% to 8% at 5.5

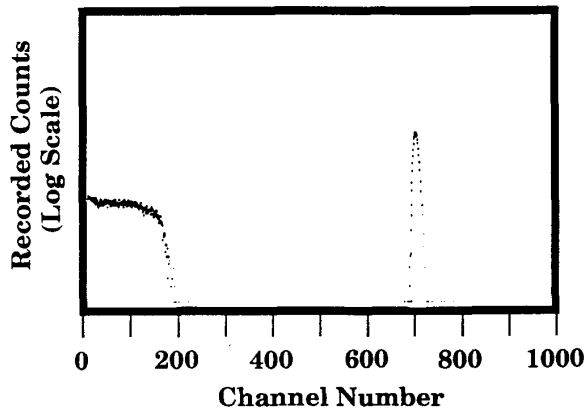

Figure 2: ^{57}Co 122 keV Gamma Ray Plateau from an Early Generation Schottky-Ohmic Bulk GaAs Detector (the sharp peak is from a pulse generator signal).

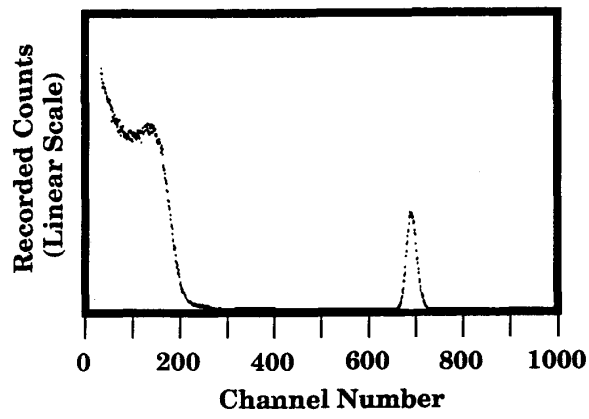

Figure 3: ^{137}Cs Beta Particle Continuum and Conversion Electrons from an Early Generation Schottky-Ohmic Bulk GaAs Detector (the sharp peak is from a pulse generator signal).

MeV. Noise was further reduced to 40 keV in later generation devices by passivation with SiO_2 or Si_3N_4 thin films.

C. *Current Effort*

Devices under present investigation utilize proton implantation to create traps and reduce carrier lifetimes on the surface. A Ti/Au Schottky contact is used as a blocking barrier under reverse bias. The blocking barrier prevents excess current from flowing into the device under reverse bias conditions. An alloyed Au/Ge/Ni ohmic contact is used to provide efficient carrier extraction while reducing statistical fluctuations. Plasma enhanced chemical vapor deposited (PECVD) Si_3N_4 films are used to passivate surface states to help reduce current leakage.

Recent efforts have been directed towards understanding the bulk GaAs material in order to correctly implement improvements for future generation devices. Thin detectors (45 microns and 100 microns in thickness) were fabricated for the purpose of investigating the active region thickness with changing reverse bias. Devices of greater thicknesses were fabricated to examine carrier lifetimes in the bulk GaAs crystal.

II. Detector Fabrication

Undoped LEC GaAs wafers were diced into 5.08 x 5.08 mm squares and polished to average thicknesses of 45 microns, 100 microns, and 250 microns. Si_3N_4 was plasma deposited onto the bare surfaces to provide passivation. Circular 4.32 mm diameter regions were etched to the bare GaAs surfaces. Afterwards, a series of alternating Au, Ge, and Ni layers were deposited in the etched region to form ohmic contact to the bare GaAs surface. The opposite side

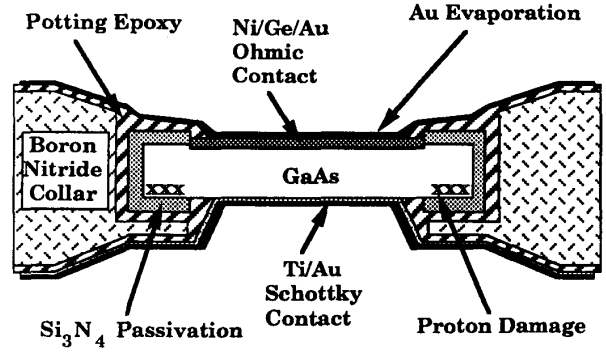

Figure 4: Bulk GaAs Detector Device Cross Section.

(front) of the crystals were polished and photoresist was patterned to protect a 4.32 mm diameter region. The front sides were implanted with protons at a dose of $10^{16}/cm^2$. Si_3N_4 was deposited over the front sides and 4.32 mm diameter regions were etched to the undamaged bare GaAs surfaces. Each piece was bonded into a boron nitride (BN) collar with high resistivity potting epoxy. Each BN collar was subsequently bonded into a pair of brass connector rings. A layer of Ti/Au was evaporated onto the front of the devices to form Schottky contacts. A final layer of Au was evaporated over the ohmic contact detector faces to form electrical contact to the connector rings. A cross section diagram of a device is shown in Figure 4 and a photograph of two finished devices can be seen in Figure 5.

Figure 5: GaAs Detectors.

III. Detector Characteristics

A. *I-V and C-V Measurements*

The forward current density due to thermionic emission from a Schottky diode can be represented by

$$J(V) = J_{st}(e^{Vq/NkT} - 1) \tag{4}$$

where

$$J_{st} = A^* T^2 e^{-\phi q/kT} \tag{5}$$

and V is the applied forward voltage, q is the charge of an electron, k is Boltzmann's constant, T is the temperature in Kelvin, A^* is the effective Richardson constant, ϕ is the Schottky barrier height, and N is the ideality factor of the current behavior [16]. Pure thermionic emission is demonstrated for diodes with an ideality factor equal to unity. The GaAs detectors displayed rectifying behavior with measured values of ideality factors ranging from 5 for thin diodes to over 40 for thick diodes. The high values of N indicate that the forward current observed is due to mechanisms other than simple thermionic emission. The turn-on voltage for forward bias current was observed to increase dramatically with detector thickness. The reverse breakdown voltage exceeded 60 volts for 45 micron thick detectors, 110 volts for 100 micron thick detectors, and 300 volts for 250 micron thick detectors.

Figure 6 shows the characteristic *I-V* curves for detectors of several thicknesses. As seen in Figure 6a, the forward bias turn-on voltages increase with detector thickness. By comparison to ideal Schottky contact diodes, the forward bias currents are slow rising. The slow rising forward currents and thickness-dependent turn-on voltages are characteristics typically found in space charge limited, trap-filled insulating materials [17]. The reverse bias current characteristics can be seen in Figure 6b. The reverse leakage current does not appear to have a thickness dependence as does the forward current. Leakage currents at 100 volts

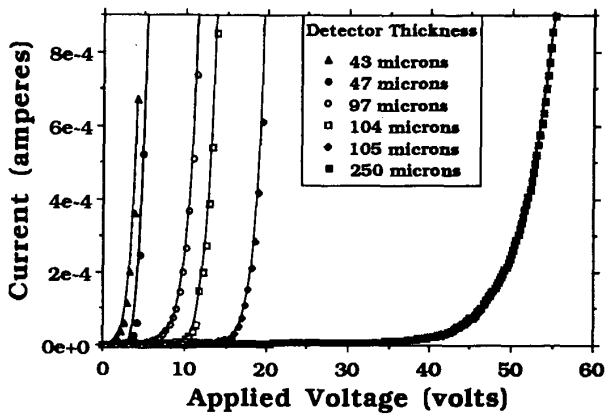

(a)

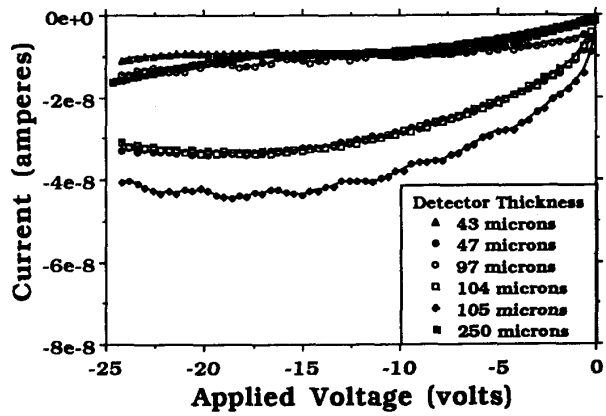

(b)

Figure 6: Characteristic *I-V* Curves for Several Thicknesses of Bulk GaAs Diode Detectors Showing the (a) Forward Currents and (b) the Reverse Leakage Currents.

reverse bias ranged from 28 nA to a worst case of 500 nA for detectors of several different thicknesses. The average reverse current at 100 volts reverse bias was 45 nA.

C-V measurements of the devices were taken with modulating frequencies ranging from 1 Mhz down to 1 Khz. In all cases, the capacitance measured showed no change with increasing reverse bias. The conductance was observed to decrease slightly with increasing reverse bias and the phase angle decreased as the frequency was lowered. Generally, the display of constant capacitance with changing reverse bias on a semiconductor indicates full depletion of the devices. However, *C-V* measurements on high resistivity material have been shown to give erroneous results [18, 19]. In a modulated *C-V* measurement, it is often assumed that capacitance is the only significant element in the circuit and the out of phase current measured on a capacitance bridge yields the true capacitance as a function of depletion layer width. In reality, diodes have a resistance between

the rectifying contact and the ohmic contact.

The small signal model of a reverse biased diode is depicted in Figure 7a. The depleted region has resistance (R_D) in parallel with capacitance (C_D), and the undepleted region also has resistance (R_S) in parallel with capacitance (C_S). The impedance across the diode is described by

$$Z = \left[\frac{R_D}{1 + j\omega R_D C_D} + \frac{R_S}{1 + j\omega R_S C_S}\right] \quad (6)$$

where ω is the modulation frequency. The value of R_D is very high and the depletion region appears mainly capacitive. In a semiconductor, the value of R_S is low enough such that C_S is shorted and the undepleted region appears mainly resistive. A common model for such a case is a capacitor (C_D) in series with a resistor (R_S) as shown in Figure 7b. If the series resistance is very high, the phase angle decreases to very small values and it can become difficult to accurately measure the capacitive component of the current.

However, the high resistance in the undepleted region of semi-insulating GaAs does not short the capacitance for the range of modulation frequencies used. If both R_S and R_D are very large, both the depleted region and the undepleted region appear to be two capacitors in series. In the limit that the high resistivity in the undepleted region becomes comparable to the high resistivity in the depleted region ($\rho_D \approx \rho_S$), equation 6 reduces to

$$Z \approx \left[\frac{\rho L_D + \rho L_S}{A(j\omega\rho\epsilon_s + 1)}\right] \quad (7)$$

where L_D is the thickness of the depletion region, L_S is the thickness of the undepleted region, A is the detector area, and ϵ_s is the dielectric constant. The current is described by

$$I \approx V\left[\frac{1}{(R_D + R_S)} + j\omega C_T\right] \quad (8)$$

where C_T is the series combination of C_D and C_S and is equivelent to the parallel plate capacitance between the Schottky contact and ohmic contact. Equation 8 is the solution to the parallel conductance circuit shown in Figure 7c. As a result, the diode appears to have a constant capacitance (C_T) between the Schottky contact and the ohmic contact in parallel with the resistances in the depleted and undepleted regions.

In reality, a low free carrier concentration is present in the undepleted region ($< 10^7$/ cm^3). Under applied voltage, the depleted region increases and the undepleted region decreases. Since the resistivity is higher in the depletion region than in the undepleted region, the overall effect is an increase in the total resistance ($R_D + R_S$), which serves to explain the experimentally observed decrease in conductance. The phase angle is described by

$$\theta = \tan^{-1}[\omega C_T(R_D + R_S)]. \quad (9)$$

Equation 9 indicates that lowering the modulation frequency causes the phase angle to decrease, which correlates with experimentally observed results. Calculated values using the model in Figure 7c closely match observed measurements. Unfortunately, since the capacitance corresponds to the total detector volume and does not change, the capacitive component yields no information concerning the depletion region thickness dependence on applied voltage.

It is also believed that the lifetimes associated with the native defect deep donor level EL2 present in the material are much too long to follow the modulated signal [16, 18, 20]. In a modulated C-V measurement, it is assumed that a change in bias voltage creates an immediate change in impurity ionization and an immediate change in depletion thickness. Such an assumption is valid as long as the carrier emission rate is much greater than the measurement modulation frequency. For practical purposes, such a case exists for shallow dopant impurities. However, the emission rate for deep levels is much lower than the emission rate of shallow levels and it is believed that the lowest modulation frequency of the C-V meter used (1 KHz) was too rapid to observe effects from the EL2 deep levels. Consequently, the effect of the deep levels on capacitance and conductance could not be determined.

B. *Pulse Height Characteristics*

GaAs material used in this study has a free carrier concentration less than 10^7/cm^3. For practical purposes, such a low carrier concentration constitutes depleted material. However, only the region in which the electric field is strong enough to remove carriers from the device is of interest. It therefore becomes necessary to define the depleted region of interest (where the electric field is capable of extracting carriers) as the device active region.

Detectors of several thicknesses were used to examine the dependence of device active region thicknesses on bias voltage. Detectors were irradiated in vacuum from the Schottky contact (front) and from the ohmic contact (back) with a spectroscopic grade 5.5 MeV ^{241}Am alpha particle source. The range of of a 5.5 MeV alpha particle in GaAs is calculated to be 20.2 microns with a straggle of 0.45 microns [21]. For a 100 micron thick detector, the electron-hole pairs will be created closest to the contact that is irradiated. However, since an alpha particle loses most of its energy near the end of its penetration distance, the expected result is a high density of electron-hole pairs created near the middle of a 45 micron thick detector whether irradiated from the front or the back.

The pulse height characteristics of a 105 micron thick detector irradiated either from the front or the back can be seen in Figure 8. A rapid increase in pulse height is observed when the detector is irradiated from the front. The bias voltage at which 95% of the maximum pulse height is observed is approximately 50 volts. Above 60 volts, the pulse height reaches a plateau. When irradiated from the

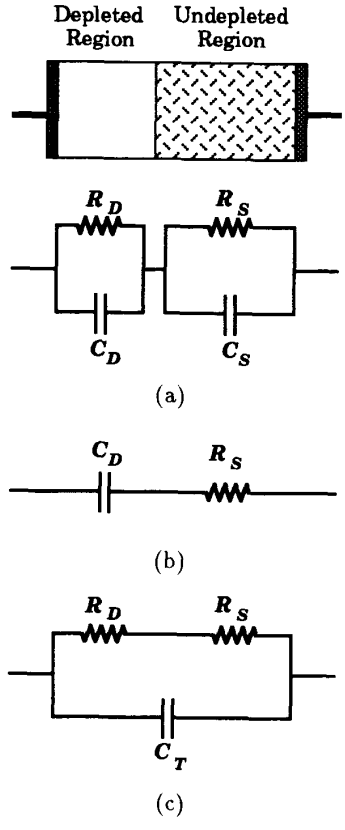

Figure 7: Small Signal Models of a Reverse Biased Diode Showing the (a) Small Signal Circuit, (b) the Series Resistance Model, and (c) the Parallel Conductance Model.

back, the pulse height only slightly increases with applied voltage at first. Near 100 volts, the pulse height rapidly increases. Beyond 130 volts, the pulse height linearly increases with bias voltage near the same saturated value as observed from front side irradiation. It is speculated that near complete electron collection is realized at a bias voltage of 130 volts. Beyond 130 volts, the linear increase in pulse height is believed to be a result of improving hole collection with increasing electric field strength.

The pulse height characteristics of a 43 micron thick detector as irradiated from the front and back can be seen in Figure 9. Again, a rapid increase in pulse height with bias voltage is seen when irradiated from the front. Similar to the 105 micron thick detector, the 95% value of the plateau pulse height was observed to occur near 50 volts bias. Similar results were found for all detectors tested independent of thickness, indicating that the electric fields near the Schottky contacts are similar for all of the detectors tested. However, when irradiated from the back, the onset of pulse height increase occurs near 50 volts for the 43 micron thick detector. In all cases, a detector thickness dependence was observed for the onset of pulse height increase when irradiated from the back. Such behavior

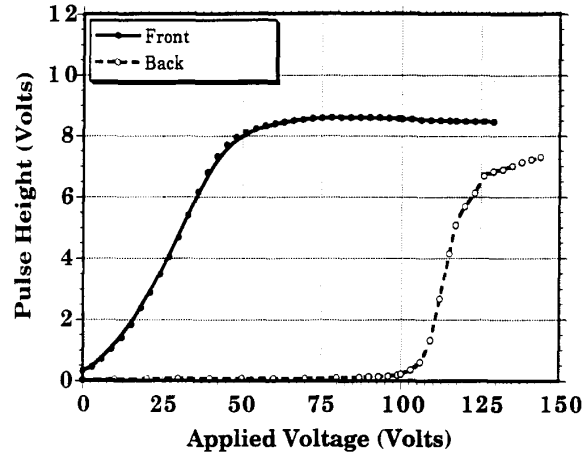

Figure 8: Measured Pulse Height as a Function of Bias Voltage from a 105 Micron Thick Bulk GaAs Detector.

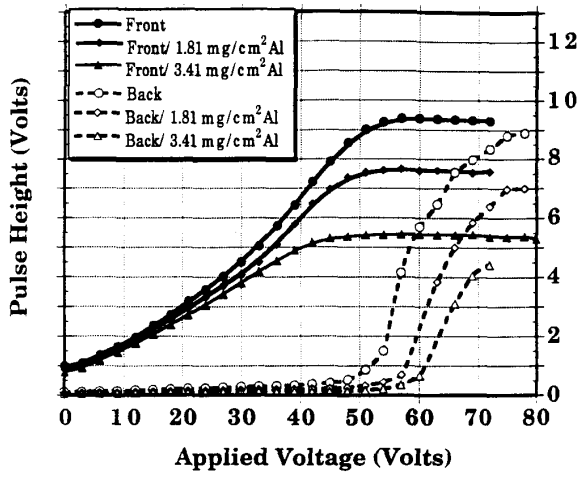

Figure 9: Measured Pulse Height as a Function of Bias Voltage from a 43 Micron Thick Bulk GaAs Detector.

is indicative of doped semiconductor material rather than intrinsic material.

Aluminum attenuators of several thicknesses were placed between the detector and the alpha particle source. The attenuators reduce the particle energy, thus reducing their range in the detector. Under front side irradiation, the plateau threshold bias voltage was observed to decrease with increasing attenuator thickness. Under back side irradiation, the bias voltage at the onset of pulse height increase was observed to increase with attenuator thickness. Full extension of the active region across the detector is realized when the pulse heights from back side irradiation saturate. The active region thickness as a function of bias voltage was determined from calculations of known particle ranges. For each alpha particle energy, the voltage at which the pulse height plateaus under front side irradiation indicates the maximum range of the particle ex-

tending from the Schottky contact. The voltage at which the pulse height abruptly increases from back side irradiation indicates the maximum range of the particle extending from the ohmic contact. The dependence of the active region thickness with bias voltage can be found by observing the necessary changes in voltage needed to arrive at each plateau or threshold value. Assuming that the voltage dependence can be described by an exponent, the dependence found is

$$W(V) \propto V^R \tag{10}$$

where $W(V)$ is the active region thickness, V is the applied reverse voltage, and R is a constant describing the voltage dependence. Values of R approached 3.5 for 45 micron thick detectors and approached 1.9 for 100 micron thick detectors. The active region width does not follow a simple $\sqrt{V}$ dependence as calculated from a one sided abrupt junction model [16].

C. *Pulsed X-ray Analysis*

To study the carrier lifetime via pulse shape, bulk GaAs detectors were exposed to fast pulses of high energy X-rays. Unlike low energy laser excitation, high energy photons create electron-hole pairs uniformly throughout the detector and allow for examination of carrier transport in the bulk crystal. The pulse duration was 50 ps with a repetition rate of 60 Hz. The current produced in the detectors was recorded using a 15 GHz sampling oscilloscope with a 50 ohm input impedance. Also recorded were the integrals of the current or the total charge collected as a function of time. Each detector tested was exposed under several bias voltages, ranging from low voltages to near breakdown. The resulting measurements clearly show two time-resolved components. The two components are most pronounced with the thickest detector tested (760 microns). Most of the charge is collected over a very short period of time (nanoseconds), whereas the tail region was observed to extend beyond 50 nanoseconds and may be due to slow hole velocities and carrier detrapping of both electrons and holes (Figure 10a). The time in which 90% of the charge is collected decreased with increasing bias voltage. For the 760 micron thick detector, the 90% charge collection time decreased from approximately 40 ns at 150 volts reverse bias to 9 ns at 750 volts reverse bias (Figure 10). Under the condition of saturated carrier velocities, 9 ns closely corresponds to the expected maximum transit time for carriers in the device. The total charge collected, Q, showed a dependence with bias voltage of

$$Q(V) \propto V^Z \tag{11}$$

where V is the applied reverse voltage and Z is a constant describing the voltage dependence. Values of Z for thick detectors ($\approx$ 750 microns) were calculated to approach 1.2 whereas values of Z for thinner detectors ($\approx$ 250 microns) approached 1.6. Since the charge deposited in the active region should be linear with respect to the active region

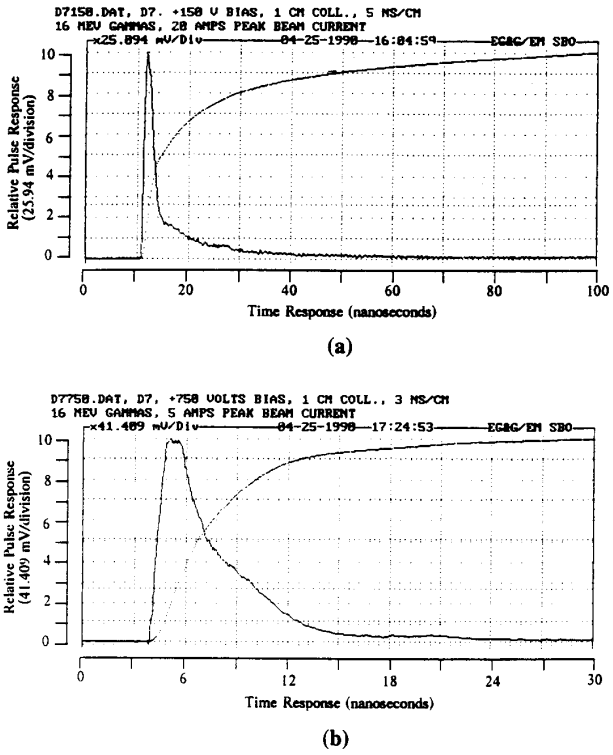

Figure 10: X-ray Pulse Response from a 760 Micron Thick Detector at a Bias of (a) 150 Volts and (b) 750 Volts.

width, the collected charge should give some indication of the active region width as a function of voltage. Similar to the pulse height analysis, a dependence was observed that deviates from $\sqrt{V}$ behavior.

D. *Alpha Particle and Gamma Ray Spectroscopy*

Spectroscopic measurements of a 5.5 MeV alpha particle source with a 105 micron thick detector resulted in a typical energy resolution of 2.5% at FWHM (Figure 11). Energy resolution for other detectors ranged from 2.2% to 3.1%. Energy resolution was observed to reach an optimum value with increasing bias voltage (Figure 12). For all detectors tested, the point at which the FWHM reached its minimum value was near the bias voltage required to reach 95% of the maximum pulse height. Assuming that ϵ = 3.65 eV/e-h pair for Si and ϵ = 4.2 eV/e-h pair for GaAs, the charge collection efficiency from front contact alpha particle irradiation as compared to a silicon surface barrier detector was 91% for a 43 micron thick detector and 82% for a 105 micron thick detector.

Room temperature measurements of 60 keV gamma rays from a ^{241}Am source resulted in a best energy resolution of 22 keV (Figure 13). Room temperature measurements of 122 keV gamma rays from a ^{57}Co source resulted in a best energy resolution of 40 keV (Figure 14). The noise level of

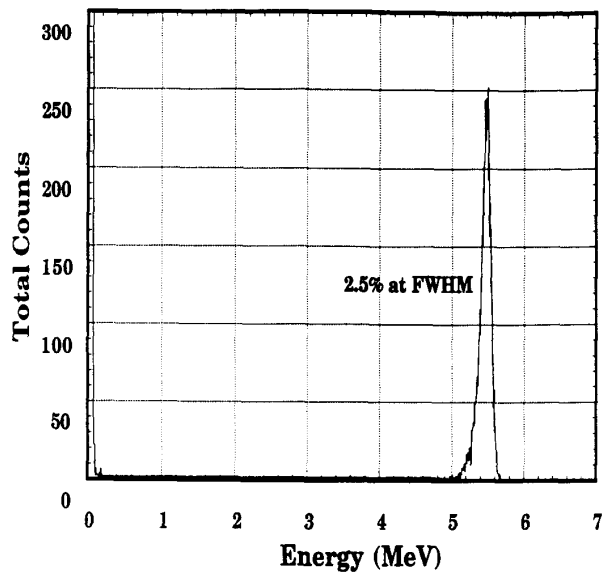

Figure 11: Pulse Height Spectrum Taken in Vacuum at Room Temperature of a 5.5 MeV ^{241}Am Alpha Particle Source with a 105 Micron Thick Detector.

these devices was measured to be 40 keV. Measurements with gamma rays of higher energy resulted in a continuum with no observable full energy peak.

IV. Discussion

Although C-V measurements show no voltage dependence on the detector capacitance, the results of the pulse height analysis with alpha irradiation clearly show an electric field dependence with applied voltage characteristic of doped semiconductors. For a uniformly doped semiconductor in which the dopants are fully ionized, the solution to a Schottky contact-semiconductor abrupt junction depletion model results in a depletion thickness that increases with $\sqrt{V}$ [16]. However, the active region thickness showed a dependence quite different from $\sqrt{V}$ behavior.

It is believed that the detector active region thickness is determined by the concentration of deep level donors and shallow acceptors[13, 22]. A simple model in which one shallow acceptor and one deep donor is present in the band gap gives

$$-\frac{\partial^2 V}{\partial X^2} = \frac{\partial E}{\partial X} = \frac{q}{\epsilon_s}(N_d^+ - N_a^- - n_o) \qquad (12)$$

where N_d^+ is the ionized donor concentration, N_a^- is the ionized acceptor concentration, and n_o is the intrinsic carrier concentration. Information supplied by the GaAs material vendor reported measured carbon concentrations on the order of $10^{14}/\text{cm}^3$ and deep donor EL2 concentrations

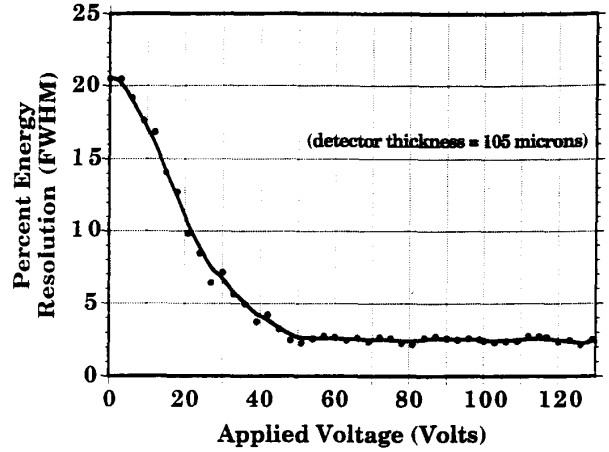

Figure 12: Energy Resolution as a Function of Bias Voltage for a 105 Micron Thick Detector.

on the order of $10^{16}/\text{cm}^3$. At room temperature, the shallow carbon acceptors are assumed to be fully ionized such that $N_a^- = N_a = 10^{14}/\text{cm}^3$. The measured energy level of the native defect deep donor EL2 is 0.8 eV below the conduction band edge [12, 23]. Assuming the Fermi level to be at midgap, the deep donors are not fully ionized and the ionized concentration of donors is

$$N_d^+ = N_{DD}\left[1 - \frac{1}{1 + \frac{1}{2}\exp(\frac{E_{DD} - E_f}{kT})}\right] \qquad (13)$$

where N_{DD} is the deep donor concentration, E_{DD} is the deep donor energy, and E_f is the Fermi energy [24]. The application of reverse voltage causes the conduction band to bend such that the energy difference between the deep donor energy level and the Fermi energy level becomes larger. The obvious result is further ionization of the deep donor level. Thus, the ionization of the deep donors present in the bulk crystal becomes a function of the bias voltage.

The numerical solution of equation 12 with an applied reverse bias results in an ionization distribution ($|N_d^+ - N_a^-|$) and an electric field distribution (E) with two distinctively different regions (Figure 15)[25]. The solution shown in figure 15a indicates that the Schottky barrier potential causes full ionization of the deep donors at the Schottky contact and the ionization concentration is simply the deep donor concentration ($N_d^+ = N_{DD} = 10^{16}/\text{cm}^3$). Further from the contact, the deep donors are no longer fully ionized and the value of $|N_d^+ - N_a^-|$ decreases to very low concentrations. With the application of a few volts, the region of complete deep level ionization extends further into the detector bulk. Consequently, the non-uniform ionization distribution creates a two zone electric field distribution across the detectors. From figure 15b, the electric field distribution near the Schottky contact decreases rapidly with a slope of qN_{DD}/ϵ_s. At the end of this region, the deep donors are no longer fully ionized and the electric

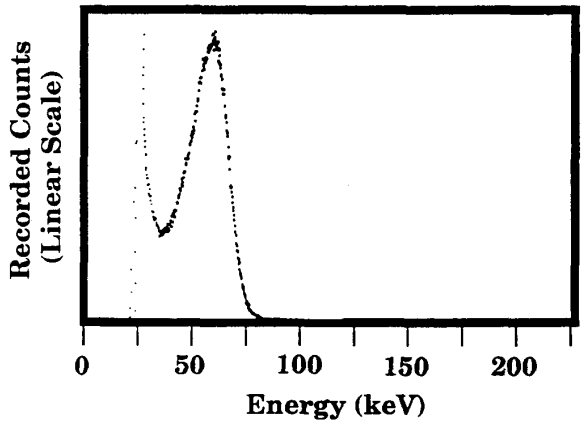

Figure 13: Room Temperature Measurement of 60 keV Gamma Rays from an ^{241}Am Source with a 250 Micron Thick Bulk GaAs Detector.

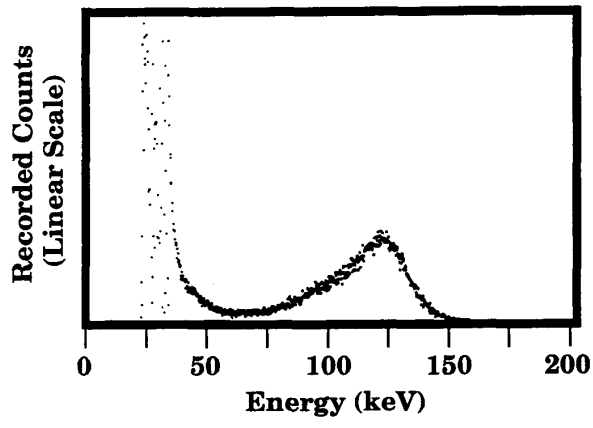

Figure 14: Room Temperature Measurement of 122 keV Gamma Rays from a ^{57}Co Source with a 250 Micron Thick Bulk GaAs Detector.

field decreases less rapidly to low values. The application of voltage causes the electric field to increase across the detector, however, the two zone electric field distribution is still present. The electric field decreases to zero at the ohmic contact. Thus, the model indicates that deep levels in semi-insulating GaAs can severely alter the electric field distribution in the detectors. Also, the conditions assumed with an abrupt junction depletion approximation (uniform ionization density and complete ionization of donors) are not realized at room temperature for semi-insulating undoped LEC bulk GaAs and the one sided abrupt junction model incorrectly represents the active region thickness as a function of bias voltage.

The resulting electric field distribution translates into high hole collection efficiency near the Schottky contact. The low electric field near the ohmic contact allows for some electron collection to occur and may account for the low pulses observed from back side irradiation before the onset of abrupt pulse height increase. Hole collection is poor near the ohmic contact, improving only when the electric field near the ohmic contact is substantially high enough to allow for increased hole extraction. Electrons are less affected by the reduced electric field near the ohmic contact since they experience high mobility at low electric field strengths.

In the pulsed X-ray experiments, the current measured is due to movement of both holes and electrons in the detector active region and carrier type is not distinguishable. However, two distinct charge decay times were observed in each of the measurements. The distinction between time components was most pronounced for thick detectors (760 microns). The short decay time component was observed to be only a few nanoseconds and approximated the maximum transit time for electrons, whereas the long decay time component extended to several tens of nanoseconds and corresponded to the maximum transit time for holes. Approximately 50% of the total charge was collected within the short decay time. Therefore, we conclude that both electron and hole components are being observed. Increasing the bias voltage had a minor effect on the short decay time, but had a dramatic effect on the long decay time.

It is believed that the dependence of the charge collection with bias voltage is the result of increasing active region width, increasing hole velocities, and changes in carrier detrapping. As the active region is increased with applied bias, the maximum transit path length for the carriers is increased. In addition, the increased bias voltage gives rise to a stronger electric field throughout the device. Thus, hole velocities increase with applied bias, whereas electron velocities decrease at fields above 3×10^3 V/cm. Since the increase in hole velocity is much more strongly affected than the increase in active region thickness, the time for hole extraction is dramatically reduced with increasing bias voltage. At high bias voltages, the observed differences in the time components become less distinctive indicating that the carriers (electrons and holes) are approaching saturated velocities and suffering less trapping and detrapping effects. The overall result is faster extraction of the charge from the devices at increasing voltages. At 750 volts bias, the observed time for 90% charge extraction from a 760 micron thick detector was measured to be approximately 9 ns, corresponding very nearly to the calculated carrier transit time at saturation velocity. Thus, the pulse response time observed is believed to actually be the carrier transit time across the active region. The measurements indicate that the actual carrier lifetimes in the bulk material may be longer than (or equivelent to) the observed charge collection time (9 ns) at high bias voltage.

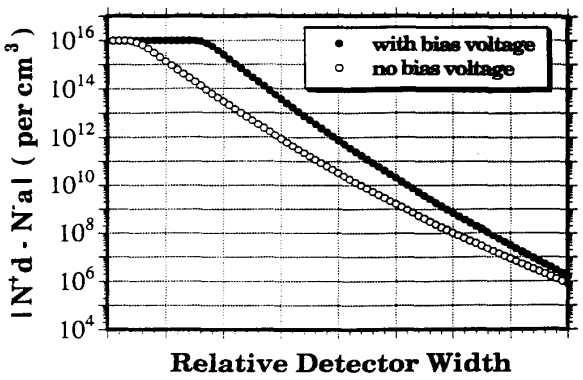

(a)

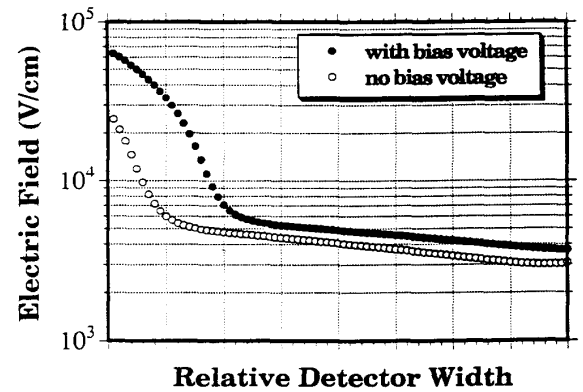

(b)

Figure 15: Numerically Analyzed (a) Ionization Concentrations and (b) Electric Field Distributions for a Simplified Model of LEC GaAs Schottky Diodes. The Fermi Energy at the Schottky Contact was Assumed to be Pinned at One Third Band Gap.

V. Conclusion

Detectors fabricated from bulk LEC undoped GaAs material resulted in the observation of 5.5 MeV alpha particles with energy resolution of 2.5% at FWHM. Also observed were full energy peaks from gamma rays of 60 keV and 122 keV energies with FWHM's of 22 keV and 40 keV, respectively. Native deep levels in the crystal are believed to cause the appearance of a two zone electric field distribution across the detector thickness. The electric field in the zone next to the Schottky contact decreases rapidly and the electric field throughout the rest of the bulk decreases less rapidly to low values. Such difficulties affect carrier extraction and pose limitations for bulk LEC semi-insulating GaAs as a high resolution spectrometer. Since semi-insulating LEC GaAs material is grown slightly arsenic rich to produce EL2 deep donor sites for carbon acceptor compensation, it is believed that an alternative bulk GaAs material to semi-insulating LEC GaAs should be used for improved results. It is felt that GaAs material with a lower overall p-type and n-type impurity concentration as well as a lower deep donor EL2 concentration may render improved results. Next generation devices will be fabricated from material with a lower concentration of carbon and EL2 levels in order to help facilitate improved electric field distributions in the device active regions. Ohmic contacts will be improved with highly doped epitaxial or implanted regions to lower contact resistance. P-I-N devices will be fabricated with improved barrier heights for gamma ray detectors.

VI. Acknowledgements

The authors wish to express their gratitude to Alan Gibbs, David Waechter, and David Brown of Los Alamos National Laboratory, William N. Gibler and Victor P. Swenson of Texas A&M University, and Ronald Rojeski, Jeff Fournier, Jim Kulman, and Jim McCartney of the University of Michigan for technical assistance in the fabrication and testing of the aforementioned devices. Proton implantation was performed by the Michigan Ion Beam Laboratory and detector fabrication was performed at the Solid State Electronics Laboratory, both located at the University of Michigan. We also wish to thank EG&G/EM in Santa Barbara for providing access to the US DOE linear accelerator.

We express gratitude towards our colleagues Dr. Fred L. Terry, Jr. and Dr. Jack East of the University of Michigan for their valued collaboration with this project.

This project has been funded in part by Los Alamos National Laboratory subcontract 9-XGO-K7910-1.

References

[1] S.P. Swierowski and G.A. Armantrout, "Prognosis for High-Z Semiconductor Detectors", *IEEE Trans. Nucl. Sci.*, NS-22, Feb., (1975), pp. 205-210.

[2] G.A. Armantrout, S.P. Swierkowski, J.W. Sherohman, and J.H. Yee, "What can be Expected from High-Z Semiconductor Detectors?", *IEEE Trans. Nucl. Sci.*, NS-24, Feb., (1977), pp. 121-125.

[3] T. Kobayashi and S. Takayanagi, "Gallium Arsenide Surface Barrier Diode as Charged Particle Spectrometer", *Nucl. Instr. and Meth.*, 44, (1966), pp. 145-146.

[4] J.E. Eberhardt, R.D. Ryan, and A.J. Tavendale, "Evaluation of Epitaxial n-GaAs for Nuclear Radiation Detection", *Nucl. Instr. and Meth.*, 94, (1971), pp. 463-476.

[5] K. Hesse, W. Gramann, and D. Höppner, "Room-Temperature GaAs Gamma-Detectors", *Nucl. Instr. and Meth.*, 101, (1972), pp. 39-42.

[6] R. Bertin, S. D'Auria, C. Del Papa, F. Fiori, B. Lisowski, V. O'Shea, P.G. Pelfer, K. Smith, and A. Zichichi, "A Preliminary Study of GaAs Solid-State Detectors for High-Energy Physics", *Nucl. Instr. and Meth. in Phys. Res.*, A294, (1990), pp. 211-218.

[7] D.S. McGregor, G.F. Knoll, Y. Eisen, and R. Brake, "Bulk GaAs Room Temperature Radiation Detectors", *Nucl. Inst. and Meth. in Phys. Res.*, in press (1992).

[8] R.N. Hall, "Recombination Processes in Semiconductors", *Proc. IEE*, 106B, Suppl. 17, (1959), pp. 923-931.

[9] J. Bardeen, "Surface States and Rectification at a Metal Semi-Conductor Contact", *Phys. Rev.*, Vol. 71, No. 10, (1947), pp.717-727.

[10] V.L. Rideout, "A Review of the Theory and Technology for Ohmic Contacts to Group III-V Compound Semiconductors", *Solid State Elec.*, Vol. 18, (1975), pp. 541-550.

[11] G.M. Martin. J.P. Farges, G. Jacob, and J.P. Hallais, "Compensation Mechanisms in GaAs", *J. of App. Phys.*, Vol. 51, No. 5, (1980), pp. 2840-2852.

[12] R.K. Willardson and A.C. Beer, *Semiconductors and Semimetals*, Vol. 20, Academic Press, Inc., Orlando, (1984).

[13] J.V. Dilorenzo and D.D. Khandelwal, *GaAs FET Principles and Technology*, Artech House, Inc., Dedham, (1982).

[14] J.E. Eberhardt, R.D. Ryan, and A.J. Tavendale, "High Resolution Nuclear Radiation Detectors from Epitaxial n-GaAs", *App. Phys. Lett.*, Vol. 17, No. 10, (1970), pp. 427-429.

[15] D.S. McGregor, R.D. White, and M.H. Weichold, "Bulk GaAs as a Room Temperature Gamma Ray Detector", *TEES Tech. Rept. Ser.*, Nov. (1985), pp. 80-90.

[16] S.M. Sze, *Physics of Semiconductor Devices, 2nd ed.*, J. Wiley & Sons, New York, (1981).

[17] M.A. Lampert and P. Mark, *Current Injection in Solids*, Academic Press, New York, (1970).

[18] D. Look, *Electrical Characterization of GaAs Material and Devices*, J. Wiley & Sons, New York, (1989).

[19] R. Stuck, J.P. Ponpon, and P. Siffert, "Behaviour of Gamma-Ray Detectors from High Purity Germanium at Low Temperature", *IEEE Trans. Nucl. Sci.*, NS-19, Feb., (1972), pp. 270-278.

[20] M. Shur, *GaAs Devices and Circuits*, Plenum Press, New York, (1987).

[21] J.F. Ziegler and J.P. Biersack, *TRIM-90*, Version 90.05.

[22] S.M. Ryvkin, L.L. Makovsky, N.B. Strokan, V.P. Subashieva, and A.Kh. Khusainov, "Preparation of Stable Counters by Means of Compensating Germanium with Radiation Produced Structural Defects", *IEEE Trans. Nucl. Sci.*, NS-15, June, (1968), pp. 226-231.

[23] Y. Kitagawara, N. Noto, T. Takahashi, and T. Takenaka, "Electron Traps in Dislocation-Free In-Alloyed Liquid Encapsulated Czochralski GaAs and Their Annealing Properties", *Appl. Phys. Lett.*, Vol. 48, No. 24, (1986), pp.1664-1665.

[24] J.P. McKelvey, *Solid State and Semiconductor Physics*, Robert E. Kreiger Publishing Company, Malabar, (1986).

[25] J. East, Private Communication, (1991).